Journal of Applied Polymer Science

Epoxy/montmorillonite nanocomposites for improving aircraft radome longevity

Carla García, Mauro Fittipaldi, Landon R. Grace
Mechanical & Aerospace Engineering Department, University of Miami, Coral Gables, Florida 33146
Correspondence to: L. Grace (E-mail: l.grace@miami.edu)

ABSTRACT: The potential of nanoclay reinforcement to improve radome performance and longevity is quantified via a resonant technique. Epoxies used for radome applications are susceptible to environmental degradation through moisture absorption. Moisture in composite systems can degrade mechanical and dielectric properties, which is of particular concern in radome applications where low dielectric properties are crucial for maintaining radar transparency. The addition of nanoclay may prove a viable method for dielectric and structural performance improvement through moisture absorption minimization. The dielectric properties of an epoxy/montmorillonite nanocomposite are evaluated as a function of nanoclay weight percentage and moisture content using a split-post dielectric resonator operating at 10 GHz. An increase of 25% in relative permittivity and 480% in loss tangent is observed for nanocomposites contaminated with 8.4% water by weight in the most extreme case. The addition of 2% nanoclay by weight effectively delayed a 16% degradation in relative permittivity by 760 hours. © 2015 Wiley Periodicals, Inc. J. Appl. Polym. Sci. **2015**, *132*, 42691.

KEYWORDS: composites; degradation; dielectric properties; nanoparticles; nanowires and nanocrystals

Received 13 March 2015; accepted 29 June 2015
DOI: 10.1002/app.42691

INTRODUCTION

In recent years, thermoset composites and nanocomposites have garnered considerable attention. The excellent mechanical properties of these polymers coupled with the vast improvement provided by low amounts of nanofillers make these composites excellent candidates for myriad applications where structural soundness and high performance are of paramount importance, such as the aerospace industry.[1–5] Within the latter, thermoset composites are primarily used as the radar-protecting structure, or radome, in aircraft-based radar systems (Figure 1). Due to their high strength, stiffness, and ability to withstand high temperatures,[6] epoxies are used in ground, marine and aircraft radome applications either as the main structural component or as coatings in radome construction. In such applications, maintaining radar transparency is crucial: The radar signal must pass unimpeded through the radome. In practical terms, this translates to choosing materials of low relative permittivity and loss tangent for radome construction, such as epoxies. However, a major drawback of these and other polymers is their susceptibility to readily absorb atmospheric moisture even in hot, dry climates.[7]

The operating environment of polymer composite radomes results in continuous exposure to moisture from humid air or precipitation in the form of water, ice or snow. The presence of water in composite systems can have a plasticizing effect on the material, acting as a crazing agent that significantly reduces both mechanical and dielectric properties.[7–11] This is of particular concern in radome applications where, as stated previously, maintaining structural integrity and radar transparency is crucial. Water present on the surface of stationary radomes in the form of thin films due to rainfall has been shown to induce transmission losses by its mere presence, and more significantly by increasing the relative permittivity of the material, which in turn leads to radar signal attenuation.[8,12–14] In addition, for ground-based radar systems, standing water layers during heavy rainfall have been shown to produce significant transmission losses, especially at higher frequencies.[13] This is not of particular concern for aircraft radomes, where precipitation causes temporary and minimal signal attenuation due to water beading and the inherent large airflow surrounding the radar structure.[12] Water present *within* the polymer network, however, can have a much more lasting and damaging effect over the service life of the aircraft, potentially resulting in permanent damage in the mechanical and dielectric properties of the material.

Over the last decade, epoxy resins have been successfully reinforced with nanoclays to produce nanocomposites with improved mechanical properties and moisture barrier capabilities intended to mitigate the deleterious effects of moisture ingress. Researchers report a substantial increase in Young's modulus, storage modulus, ultimate strength at failure, and

© 2015 Wiley Periodicals, Inc.

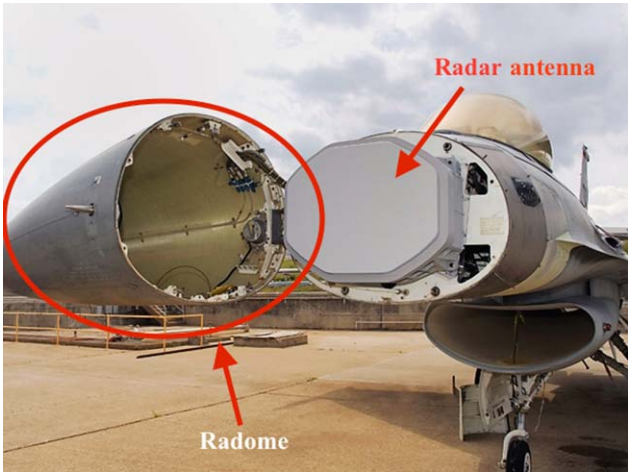

Figure 1. Aircraft radomes protect the radar antenna from environmental degradation. Water absorption and pooling within the radome can significantly attenuate the radar signal. Image courtesy of Raytheon Company. [Color figure can be viewed in the online issue, which is available at wileyonlinelibrary.com.]

thermal stability with only a small amount of nanoparticles (generally up to 5% by weight) incorporated in the polymer resin.[3–6,15–17] Of the thermoset nanocomposites, epoxy/nanoclay composites have been the most widely studied due to the ubiquitous nature of these clays, their affordability, and their unique geometries. Sheet silicates, such as bentonite (montmorillonite) clays, have a layered structure comprised of an aluminum octahedron sandwiched between two silica tetrahedrons. Each of these layers, or sheets, is approximately 1 nm thick and can be up to several microns wide. The layers are piled together to form "stacks", each layer being separated by a van der Waals gap of approximately 1.8 nm called the gallery spacing, basal spacing, or intragallery space.[15] The high aspect ratios of these clays provide a "tortuous" path for the diffusion of water through the polymer, effectively delaying moisture uptake. However, improvements in barrier properties are contingent upon proper delamination and dispersion of these clays, which is a highly challenging process and is dependent on numerous factors including clay surface treatment, the cation exchange capacity of the clays, curing rate, and clay compatibility with the resin.[18,19]

Clay nanocomposites can have one of three different types of morphologies:[15,18] microcomposite, intercalated nanocomposite, or exfoliated nanocomposite. Due to the vast increase in surface area and phase homogeneity produced in the exfoliated morphology, it is the most likely to appreciably improve mechanical properties.[20] It is also the most likely morphology to generate improvements in moisture barrier properties. Liu *et al.* reports a rapid decline in transverse diffusivity and moisture uptake rate in orderly exfoliated epoxy/clay nanocomposites with increasing clay loading up to 7.5% by weight, further stating that the higher the aspect ratio of the clays, the lower the transverse diffusivity values observed.[16]

Although the intercalation chemistry of nanoclays has been studied extensively, there is still no general consensus for a fabrication method that will produce a true exfoliated morphology. This is because complete delamination and intercalation of the clays is dependent upon many factors that are difficult to independently control. Silicate clays are naturally hydrophilic. As a result, the hydrated cations of the intragallery must be exchanged with onium cations to make them organophilic to improve compatibility with the polymer resin and to allow for intercalation with the galleries.[15] Further, although delamination is controlled by a mechanical force (shear mixing), intercalation and expansion of the intragallery space is controlled by a chemical reaction factor.[21] Hence, the choice of curing agent plays a crucial role in the final composite morphology. Due to these numerous factors involved in proper clay dispersion, in practice most nanocomposites will have, upon well dispersion of the clays, a combination of both intercalated and exfoliated morphologies.

Recent work has focused on the addition of inorganic nanofillers to epoxy resins to assess and quantify effects on dielectric properties. The incorporation of metal oxide nanoparticles has been shown to improve dielectric properties at low frequencies.[22] However, the addition of nanofillers has been shown to also deteriorate dielectric properties in some cases, with impact on dielectric properties dependent on factors such as fabrication method, type of nanoparticle, nanofiller loading, surface treatment, and frequency.[22–27] Although the effect of nanoclays on dielectric properties such as relative permittivity and loss tangent has not been thoroughly assessed in the literature, a slight reduction in these properties was reported for low frequencies (50 and 60 Hz) and low clay loadings (up to 5% by weight), and attributed to the restriction in polymer chain mobility provided by the nanoclays.[23,24,26] The objective of the present work is to determine whether nanoclays have an effect on the dielectric properties of an epoxy resin at 10 GHz (X-band), and to assess whether, through a decrease in moisture barrier properties, nanoclays can effectively delay or mitigate significant dielectric property degradation as a result of water contamination. To this end, epoxy nanocomposites were fabricated with nanoclay loadings of 1, 2, 3, and 5% by weight using an identical procedure, which was expected to produce nanocomposites of varying morphology for evaluation.[21,28–30] X-ray diffraction analyses (XRD) and transmission electron microscopy (TEM) were used to determine the degree of nanoclay dispersion and the nanocomposite morphologies. The relative permittivity and the loss tangent, which are directly related to the radar transparency of the material,[31,32] were evaluated in the dry state using a split-post dielectric resonator (SPDR) to determine the effect of clay loading percentage and morphology. Samples were then immersed in constant temperature water baths to carry out the diffusion experiments, and the relative permittivity and loss tangent evaluated as a function of moisture uptake at different time intervals.

EXPERIMENTAL

Materials

The epoxy resin used is a diglycidyl ether of Bisphenol A (EPON™ 828, supplied by Momentive™ Specialty Chemicals, Inc.). This epoxy has very good mechanical, adhesive, dielectric

and chemical resistance properties and is widely available, widely studied, and commonly used in radome construction and/or coating. The curing agent used is aminoethylpiperazine (EPIKURE™ 3200, also supplied by Momentive™ Specialty Chemicals), which was chosen because it cures at room temperature in 24 hours, thus allowing more time for the polymer chains to intrude the intragallery space and increase the basal spacing between clay platelets. The montmorillonite clay used is Cloisite® 30B, supplied by Southern Clay Products, Inc. (now a part of BYK Additives & Instruments), which is also widely available and widely studied. This clay is surface treated with a methyl tallow bis-2-hydroxyethyl quaternary ammonium.

Fabrication of Epoxy Nanocomposites

The epoxy nanocomposites were fabricated with clay loadings of 1, 2 3, and 5% by weight to assess the effect of typical nanoclay loading percentages on relative permittivity and loss tangent. Further, the fabrication method was kept consistent regardless of clay loading. This is atypical in epoxy/nanoclay systems, which generally require optimization of dispersion method based on clay loading percentage. As such, the consistent mixing method regardless of clay content was expected to result in nanocomposites of varying degrees of dispersion and exfoliation. In this study, such a range of morphologies was desired to provide insight into any potential effect of clay dispersion or exfoliation on dielectric properties.

The resin to curing agent ratio used was 100 to 22 by weight. The resin (50 g) was poured into 150 mL glass beakers and then heated to approximately 60°C over a hot plate to remove bubbles introduced in the pouring process. The nanoclay was added to the beaker and mixed by hand, followed by high shear mixing at 2000 rpm for 1.5 hours, irrespective of clay loading. The nanoclay-resin mixture was then sonicated for 15 minutes over an ice bath to prevent the resin from burning due to the high temperatures induced by sonication. The mixture was then degassed in a vacuum oven maintained at 80°C for 24 hours, or until all entrapped air had been removed. This greatly reduces the amount of nano to micro-sized voids which can ultimately prevent performance improvement.[33] After degassing was complete, the samples were allowed to cool to approximately 35°C before mixing with the curing agent.

Once mixed with the curing agent, samples were cast between two heat resistant square glass plates and clamped together, with 0.9 mm thick aluminum shims employed to maintain consistent separation between the plates and minimize sample thickness variations. The plates were first treated with Frekote® 44-NC™ Mold Release Agent as per manufacturer instructions. The samples sandwiched between the glass plates were allowed to cure at room temperature for 24 hours, followed by a 1 hour post-cure at 150°C. Once the samples were demolded, they were cut using a wet diamond saw into squares of approximately 6 cm by 6 cm. Three samples were cut for the neat epoxy and each clay loading percentage. Finally, cut and labeled samples were dried in a vacuum oven at 50°C for 48 hours, and left in a desiccator for an additional 48 hours to ensure removal of all residual moisture. Dry samples were weighed, the relative permittivity and loss tangent measured, and then immersed in containers filled with distilled water. These containers were then submerged in a water bath maintained at 25°C. The time and date of immersion was recorded.

Characterization

Nanocomposite morphologies were evaluated by small angle XRD. The radiation used was CuK_α ($\lambda = 1.54056$ Å), with a 2θ scan range from 0.02° to 9.98°. The nanostructure of the composite was assessed through TEM. Samples of 1 mm by 1 mm were embedded in a low viscosity "Spurr" resin, and thin sections of approximately 80 nm were then cut using an ultramicrotome prior to TEM characterization.

Experimental Procedures

Dielectric Property Measurements. To perform the dielectric measurements, an SPDR connected to a vector network analyzer (Agilent AT-E8362C/P1) operating at 10 GHz was used. The thickness of each sample was measured using a digital micrometer caliper. Five thickness measurements were performed at the center and four corners of each sample and averaged. The average thickness was used in the computation of the relative permittivity and loss tangent for each sample. For measurements in the dry state, samples were removed from the desiccator one at a time and five measurements per sample were taken by shifting the sample slightly within the resonator cavity. Reported dielectric properties are an average of these five measurements. Because the SPDR method is highly sensitive to thickness variations, this was done to account for the minutely varying thickness of each sample. At predetermined time intervals after immersion, samples were removed from the water bath one at a time and dried using a lint-free cloth. The dielectric properties were measured immediately after drying, again taking and averaging five measurements for each sample.

Gravimetric Moisture Uptake Measurements. Gravimetric moisture uptake was monitored via a high precision analytical balance. Samples were removed from immersion one at a time and dried using a lint-free cloth. Weight was recorded immediately after measuring the dielectric properties for each sample. The samples were then re-immersed in the water baths, and the procedure was repeated for the neat epoxy and for each clay loading percentage. Total immersion time was recorded for all samples.

RESULTS AND DISCUSSION

Nanocomposite Morphology

As expected, a range of nanocomposite morphologies were produced by varying clay content without adjusting the fabrication method. These morphologies were characterized using the standard procedure of XRD and TEM. In this case, characterization by these methods indicated that the 2% clay/epoxy system most likely contains the most effectively dispersed nanoclay. As a result, this system is expected to exhibit the most significant improvements in mechanical properties and moisture barrier performance.

To arrive at this conclusion, XRD was used to determine gallery spacings using a simple form of Bragg's equation:

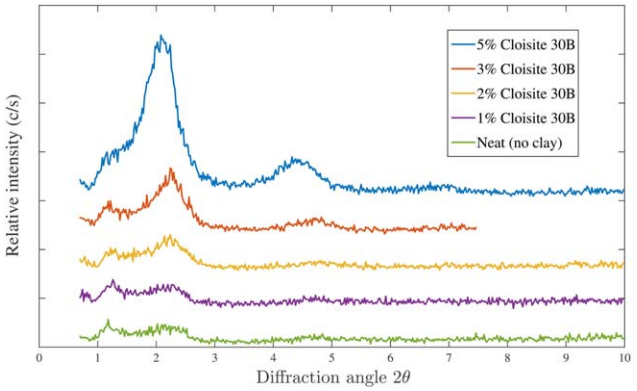

Figure 2. XRD patterns for nanocomposites. Peaks are indicative of intercalated morphologies. [Color figure can be viewed in the online issue, which is available at wileyonlinelibrary.com.]

$$\lambda = 2d \sin\theta \quad (1)$$

where λ is the radiation wavelength, d is the gallery space, and θ is the diffraction angle. The presence of peaks in the XRD pattern indicates ordered-intercalated and/or ordered-exfoliated nanocomposites.[21] Figure 2 shows the XRD patterns for the nanocomposites, with all samples showing a peak corresponding to a 2θ angle of approximately 2.2°. Using eq. (1), these peaks correspond to an increased basal spacing of approximately 3.87 nm, 3.80 nm, 3.94 nm, and 4.24 nm respectively, in order of increasing clay loading. These basal spacings are consistent with the literature and are indicative of an ordered-intercalated morphology.[20,21,34] For the lower clay loadings, this peak is quite small, however it is much more prominent for the higher clay percentages. Generally, an exfoliated nanocomposite will exhibit basal spacings greater than 8 nm, with values up to 240 nm reported for fully exfoliated structures.[20,34]

Additionally, for the higher clay loadings, a smaller peak is observed at a 2θ angle of around 5°. This peak is representative of the peak observed in the pure clay diffraction pattern (at approximately 4.8°)[35] and is indicative of clay agglomerates present in the nanocomposites. This simply means that the clay was not sufficiently delaminated, i.e., stacks may have remained intact and no polymer likely intruded the gallery spacing. The presence of agglomerates at higher clay percentages is quite common.

TEM is normally performed in conjunction with XRD to determine the degree of intercalation and/or exfoliation and whether the clay platelets are ordered or randomly oriented within the resin. Figure 3 shows TEM images at low magnification for all clay loadings. While all images depict some degree of ordered intercalation, the 2% clay sample appears better intercalated than the rest. The high magnification images shown in Figure 4 more effectively illustrate the higher degree of intercalation exhibited by the 2% sample. Darker areas indicate the intersection of individual silicate sheets,[21] and are more prominent in the 1, 3, and 5% clay samples. These areas also indicate the presence of agglomerates, where each silicate sheet was minimally sheared from its "stack" or not properly delaminated, and the basal spacing was not uniformly increased. Although a higher aspect ratio and clay volume fraction are desirable for a reduction in transverse diffusivity and moisture uptake rate, the presence of agglomerates produces the same effect as reducing the aspect ratio of the clays. That is to say, the rate of reduction in transverse diffusivity for the other clay loadings may be in fact much lower due to the presence of large amounts of

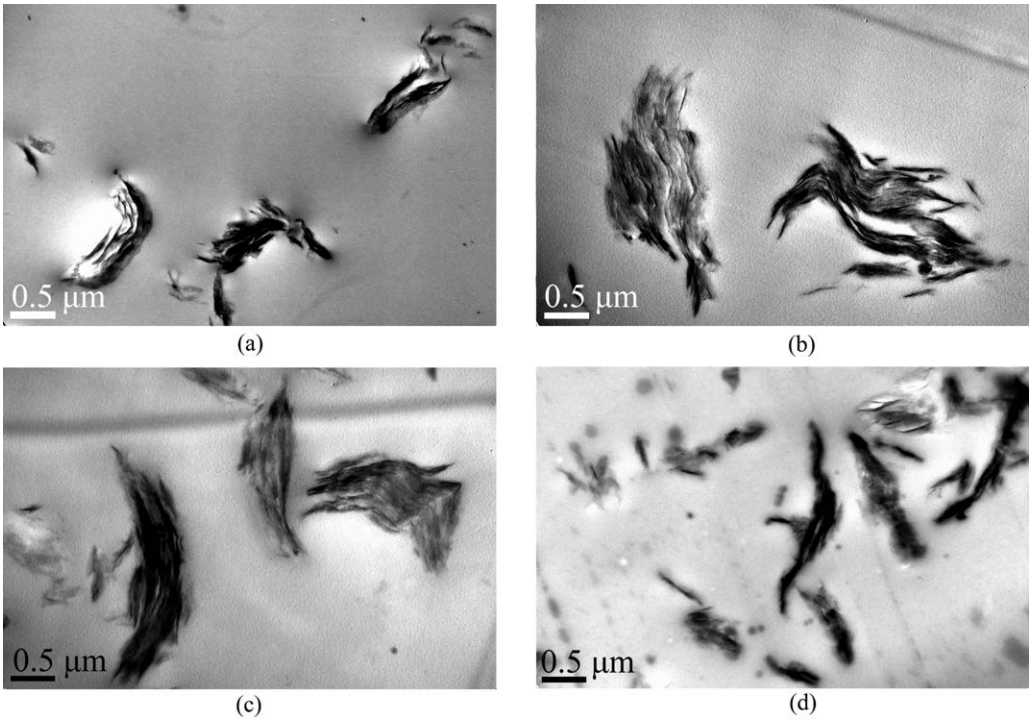

Figure 3. Low magnification (25,000×) TEM images: (a) 1%; (b) 2%; (c) 3%; (d) 5% clay loading percentages.

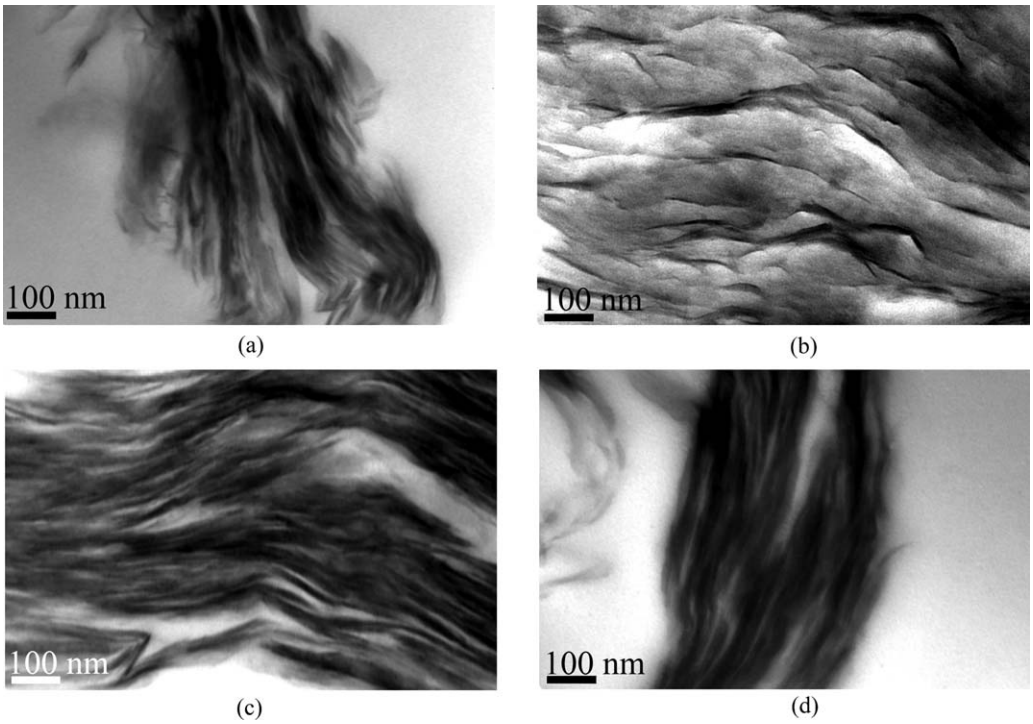

Figure 4. High magnification (130,000×) TEM images: (a) 1%; (b) 2%; (c) 3%; (d) 5% clay loading percentages.

agglomerates, despite intercalation of the clay platelets.[16] Based on the higher degree of intercalation observed in the 2% sample, it is expected to offer the greatest improvement in moisture barrier properties by providing a wider intragallery space wherein the diffusion of water molecules might be effectively delayed.

In summary, characterization showed that the chosen fabrication method resulted in the most desirable morphology for the 2% nanoclay/epoxy system. Besides moisture barrier property improvement, it is postulated that any potential improvement in dielectric properties would be seen in this system as opposed to the other clay loadings. Such a result would be consistent with the slight improvement in these properties observed at low frequencies and low clay loading percentages, which has been attributed to the restriction in polymer chain motion provided by the clays.[23,24,26]

Dielectric Properties in the Dry State

The resonance method used in this study for dielectric property characterization is a highly accurate and convenient method that uses an SPDR fixture connected to a vector network analyzer to compute the real part of the relative permittivity and loss tangent of a thin, laminar sample.[36] The schematic of the fixture used is shown in Figure 5. The relative permittivity and loss tangent of a thin dielectric material is calculated using the shift in resonant frequency and Q-factor due to the presence of a specimen in the resonator. To compute the real part of the relative permittivity, ε', of a sample, the following equation is solved iteratively:

$$\varepsilon'_r = \frac{1+f_0-f_s}{hf_0K_s\left(\varepsilon'_r, h\right)} \tag{2}$$

where h is the sample thickness, f_0 is the resonant frequency of the empty SPDR, f_s is the resonant frequency of the SPDR with the dielectric sample, and K_s is a function of the sample relative permittivity and thickness. K_s is computed and tabulated for every specific SPDR.

Similarly, to compute the loss tangent of the material (also known as tan delta, tangent loss, or dissipation factor), the following equation is used:

$$\tan\delta = \frac{Q^{-1}-Q_{DR}^{-1}-Q_c^{-1}}{P_{es}} \tag{3}$$

where Q is the unloaded Q-factor of the resonator containing the dielectric sample, and p_{es} is the electric energy filling factor of the sample.

Typical uncertainty using an SPDR for calculation of the relative permittivity is ±1 percent, given that the thickness of the sample is measured with an accuracy of ±0.7 percent or better. The principal source of uncertainty in measurements of the real permittivity is related to uncertainty in thickness measurements, with the relative error due to thickness uncertainty equivalent to:

$$\frac{\Delta\varepsilon'_r}{\varepsilon'_r} = T\frac{\Delta h}{h} \tag{4}$$

Where $1 < T < 2$. Normally, T is close to unity except for thick, large permittivity samples.[37] Hence, to reduce the error associated with calculating the relative permittivity, it is imperative that samples be of a consistent thickness throughout, and that a micrometer caliper be used to ensure accurate thickness measurements.

The incorporation of nanoclays did not adversely affect the relative permittivity or loss tangent of the epoxy nanocomposites in the dry state. Figures 6 and 7 show the relative permittivity and loss tangent as a function of clay loading. The 5% clay sample shows an increase (deterioration) in the relative permittivity

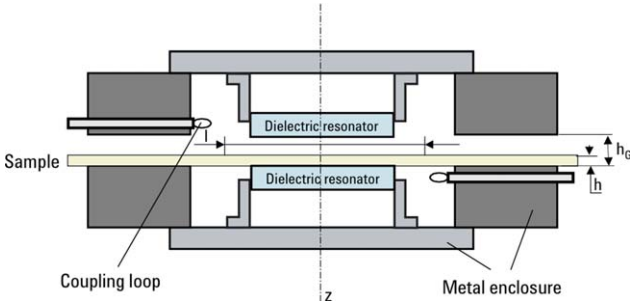

Figure 5. SPDR fixture for dielectric property measurements. [Color figure can be viewed in the online issue, which is available at wileyonlinelibrary.com.]

compared to the neat sample. However, this value is representative of only a 0.36% deterioration. Conversely, the 1% clay sample shows an improvement of 0.42% in relative permittivity compared to the neat sample. When considering the importance of accurately measuring the thickness of the samples and the thickness sensitivity of the method used for calculating the relative permittivity as seen in eq. (4), these slight fluctuations in the reported values may well be attributed to thickness variations from sample to sample. Despite a concerted effort to minimize thickness variations, samples cast between the plates varied in thickness from edge to edge by as much as 90 microns in some cases. These inconsistencies, while small, may be significant enough to cause a change in the calculated relative permittivity. Regardless of this potential source of error, it is clear that the addition of nanoclays does not appreciably affect the relative permittivity of the epoxy. A similar trend is observed for the loss tangent in the dry state. In fact, the addition of nanoclays can be said to modestly improve the loss tangent values: For the most extreme case (the 2% clay sample), the loss tangent improved by 13% when compared to the neat sample. As mentioned previously, this is likely due to the more effectively intercalated/exfoliated morphology of the 2% clay sample, which may result in restricted polymer chain motion and a reduced loss tangent.

Gravimetric Moisture Uptake

Moisture uptake curves are plotted in Figure 8. The reported values represent the average of all three samples for the neat case and for each clay loading. Only the 2% clay nanocomposite

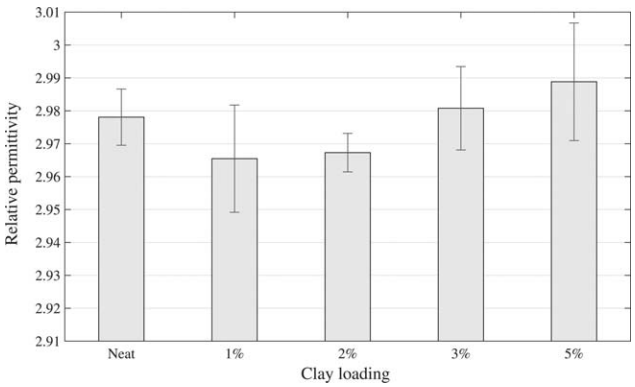

Figure 6. Relative permittivity as a function of clay loading. Error bars depict a 95% confidence interval.

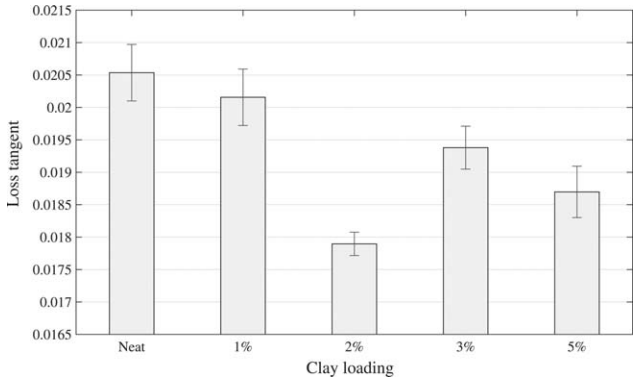

Figure 7. Loss tangent as a function of clay loading. Error bars depict a 95% confidence interval.

exhibits a decrease in water uptake rate and a decrease in equilibrium moisture content when compared to the neat sample. The 1% clay sample shows a slight increase in total moisture content, while the 3 and 5% clay samples fall slightly above the 1%. The best-fit curves corresponding to the one-dimensional isotropic Fickian diffusion model for the neat and 2% clay samples are plotted in Figure 9. The Fickian mass gain is given by the following equation:[16]

$$\frac{M_t}{M_\infty} = 1 - \sum_0^\infty \frac{8}{(2n+1)^2\pi^2} \exp\left[\frac{-D(2n+1)^2\pi^2 t}{h^2}\right] \qquad (5)$$

where M_t and M_∞ are the mass uptake percentages at time t and at equilibrium, respectively, D is the diffusion coefficient, and h is the sample thickness. Fickian curves were plotted against the experimental data and the diffusion coefficients calculated from eq. (5) using a least squares regression. Although the experimental data does not exactly obey Fick's Law, this law is widely used to calculate polymer diffusivities since water uptake in polymers is linearly proportional to the square root of immersion time in the initial stages.[16] Calculated diffusivities are shown in Figure 9.

The behavior observed in Figure 9, wherein only the 2% clay samples show enhanced barrier properties, can be attributed to several factors and is consistent with expectations based on the

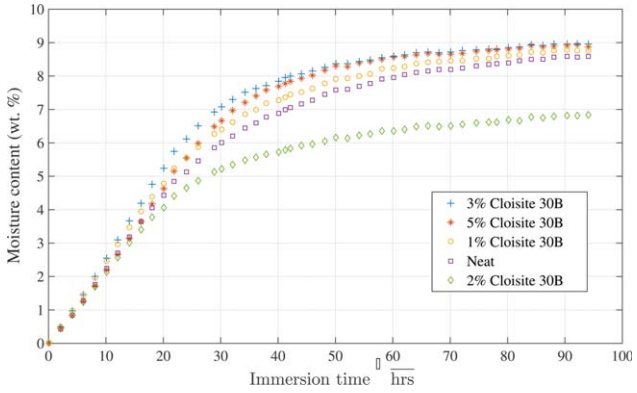

Figure 8. Moisture content as function of immersion time. [Color figure can be viewed in the online issue, which is available at wileyonlinelibrary.com.]

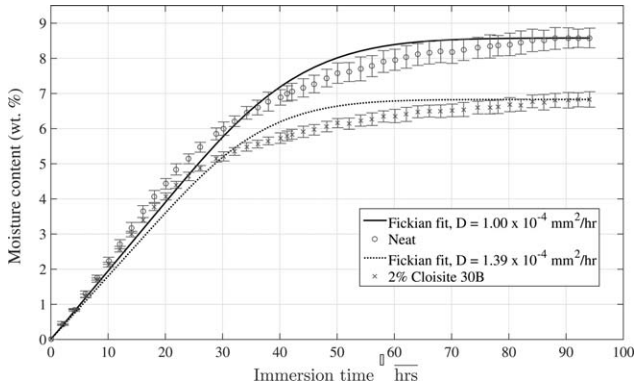

Figure 9. Neat and 2% clay sample water uptake curves. Fickian curves were plotted against the experimental data to calculate diffusion coefficients. Error bars depict a 95% confidence interval.

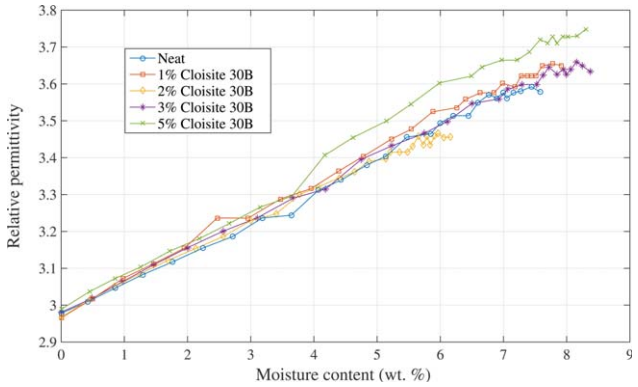

Figure 10. Relative permittivity as a function of moisture content. [Color figure can be viewed in the online issue, which is available at wileyonlinelibrary.com.]

morphology characterization. The morphologies of the nanocomposites show partial ordered exfoliation at best for the 2% clay samples, with ordered intercalates observed in the 1%, 3%, and 5% clay samples. At the forefront, improper clay dispersion (especially for the higher clay loadings) may accurately explain the observed behavior. However, the overall orientation of the clays within the polymer likely plays a crucial role. Based on the TEM images, there is no clear evidence as to the orientation of all the clay platelets within the composites. However, as observed by Liu *et al.*, nanoclays have no influence on the diffusivity of the nanocomposites in the direction parallel to the clay platelets. In contrast, they have a great influence on the diffusivity and moisture uptake rate in the direction normal to the face of the clay platelets by providing a "tortuous" path for the diffusion of water molecules around the platelets.[16] Hence, the slightly more intercalated/exfoliated morphology seen in the 2% clay sample likely contributed to the enhanced moisture barrier properties observed by providing more surface area (a higher "tortuosity" factor) for the diffusion of water molecules to be effectively reduced.

The increase in equilibrium moisture content with increasing clay loading has been studied previously using treated and untreated clays.[3,6,8,16] Untreated clays have been shown to increase both transverse diffusivity and maximum water uptake due to the hydrophilic nature of the clays. Treated clays, however, do not normally exhibit this behavior, although increases in equilibrium moisture content have been reported and attributed to the growth of the interphase weight content at higher clay loadings.[6] Pontefisso *et al.* studied the influence of the interphase layer on the elastic properties of nanoparticle filled polymers. Although they modeled spherical silica nanoparticles, the presence of an interphase layer surrounding the nanoparticle with properties differing from the nanofiller and the polymer matrix is worth noting.[38] The geometry of this interphase layer may be quite complex and unique for layered silicates, yet it is worth mentioning that the water content in this interphase at the higher clay loadings may be significant enough to contribute to the observed moisture uptake dynamics.

Furthermore, the incorporation of nanoclays in an epoxy resin has been shown to increase free volume and micro-voids when compared to the neat resin.[17] This can create a negative feedback loop when water is introduced to the resin by accelerating moisture diffusion and increasing equilibrium moisture content through the additional mass transport associated with these inherent micro-imperfections, which are in turn further exacerbated by moisture ingress.[3] In practice, a combination of all these factors may have contributed to the observed moisture uptake dynamics. Importantly, the 2% clay sample exhibits ideal behavior and, even though it has a slightly higher diffusivity, the maximum moisture uptake rate and equilibrium content for the sample are significantly lower than that of the neat resin, as expected. The slightly higher diffusivity is simply a result of the dependence of this parameter on equilibrium moisture content, which is considerably lower for the 2% clay sample.

Dielectric Properties in the Water-Contaminated State

Figures 10 and 11 show the relative permittivity and loss tangent as a function of moisture content, respectively. For both cases, a consistent increase (degradation) in dielectric properties is observed, with a total degradation in the relative permittivity and loss tangent of 25% and 280%, respectively, for the most extreme case. Although the effects on the dielectric properties due solely to the incorporation of the nanoclays are nearly negligible, the deleterious effects induced by the presence of absorbed water are much more prominent, as expected. For all clay loadings, a nearly direct correlation can be observed

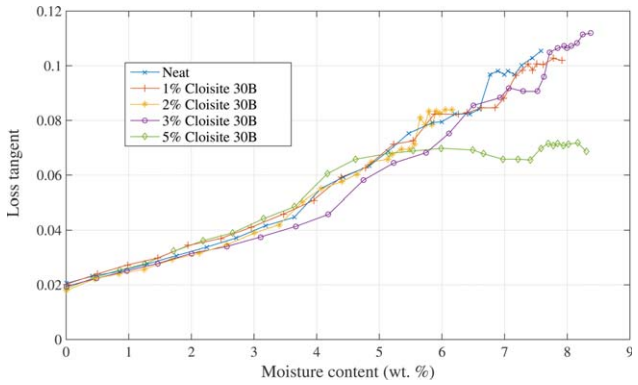

Figure 11. Loss tangent as a function of moisture content. [Color figure can be viewed in the online issue, which is available at wileyonlinelibrary.com.]

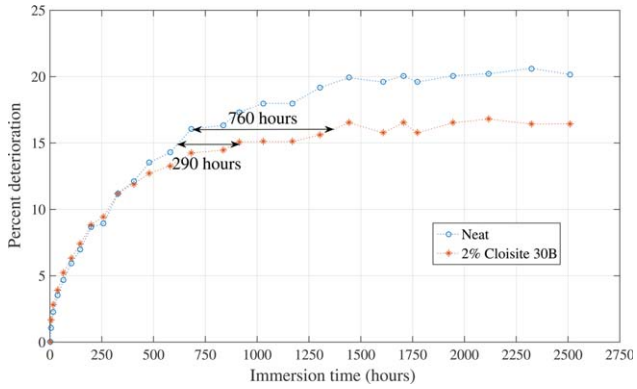

Figure 12. Percent deterioration in relative permittivity for the neat and 2% clay samples plotted against total immersion time in hours. [Color figure can be viewed in the online issue, which is available at wileyonlinelibrary.com.]

between dielectric property degradation and moisture content, regardless of clay weight percentage. For example, at 2% moisture content, the relative permittivity and loss tangent are nearly equivalent for all clay loading percentages. This result suggests that the interaction of the oscillating electromagnetic field with water present in the nanocomposite completely overshadows any dielectric effect of the clay. This result is not surprising, given the very high relative permittivity (~80) of liquid water at X-band.

The presence of water within composite radome structures is most likely the result of precipitation, condensation, humid air, or standing water within an improperly sealed radome in the most extreme case. The scenario described in the present work most closely represents this most extreme case. The practical result of this or any type of real-world moisture exposure is a fluctuating total moisture content within the material comprised of alternating absorption/desorption cycles coupled with a baseline moisture content. In delaying moisture uptake, the addition of nanoclay may promote a lower baseline moisture content and a lower maximum moisture content relative to the neat epoxy.

To further illustrate this point, Figure 12 shows the percent deterioration in relative permittivity plotted against immersion time for the neat and 2% clay samples. In the initial stages, nearly no delay in degradation is observed. For higher immersion times, however, the delay in degradation is significant. For example, a 15% degradation in relative permittivity was delayed by 290 hours through the addition of nanoclay. Likewise, a 16% degradation was delayed by approximately one month (760 hours). These delays are largely restricted to the upper end of total moisture content. This is especially significant for the worst-case (and relatively common) scenario wherein water pools within a radome interior. In such a situation, water absorption will be rapid and significant. The addition of nanoclay may delay dielectric property degradation long enough to allow removal of standing water through evaporation or via maintenance operation. In addition, the total relative permittivity increase at equilibrium is much lower for the 2% nanoclay-reinforced epoxy. These samples, unlike the neat epoxy, never reach a 20% degradation in relative permittivity. This improved dielectric performance suggests that nanoclay-reinforced epoxy radomes may significantly improve radar performance and longevity.

CONCLUSIONS

Epoxies used in radome applications are susceptible to degradation due to environmental effects, particularly moisture absorption. Moisture in thermosetting polymers has been shown to negatively impact the material's mechanical and dielectric properties. In recent years, high aspect ratio silicate sheets have been shown to not only improve the polymer's mechanical properties, but also to effectively decrease the moisture diffusion rate. However, these improvements are dependent on the degree of nanoclay dispersion and the formation of an exfoliated nanocomposite.

In this study, the viability of using nanoclays for mitigating or delaying significant dielectric property degradation was quantified and assessed. Epoxy samples were fabricated with up to 5% clay content by weight and submerged in a water bath maintained at 25°C. Nanoclay dispersion was determined by small angle XRD and TEM, and was found to be most effective in the 2% nanoclay samples. The dielectric properties were measured in the dry state and at different moisture contents using a SPDR connected to a vector network analyzer operating at X-band (10 GHz). The XRD and TEM characterization revealed ordered-intercalated composites, with a partially exfoliated morphology seen in the 2% clay sample. Due to the lack of complete clay exfoliation in all samples, moisture absorption reduction was only observed for the 2% clay content sample.

Relative permittivity and loss tangent were not measurably affected by the addition of nanoclay, providing sound evidence that this reinforcement option will not sacrifice radar performance. These values significantly increased with increasing moisture content, regardless of clay content. In the worst case, relative permittivity and loss tangent increased by 25% and 480%, respectively. However, epoxy samples reinforced with 2% clay content by weight exhibited improved water barrier properties when compared to the neat epoxy and improved dielectric properties in the water-contaminated state. More importantly, the degradation in dielectric properties was significantly delayed temporally, thereby prolonging usable service life and likely reducing baseline water content. Water-contaminated neat epoxy exceeded 20% degradation in relative permittivity, while 2% clay epoxy samples showed a worst-case degradation of approximately 16% within the experimental time frame. Further, this level of degradation was delayed by more than one month for the 2% clay sample at longer immersion times, which are representative of worst-case standing-water scenarios. Therefore, nanoclays appear to be excellent filler options for epoxy radomes. The moisture barrier benefits provided may prolong radome longevity by effectively reducing and delaying significant dielectric property degradation without affecting the dry-state performance.

ACKNOWLEDGMENTS

The authors acknowledge the support of Chugach, Inc. and the United States Air Force (W15P7T-09-D-S609) for partial support of this study.

REFERENCES

1. Bekyarova, E.; Thostenson, E. T.; Yu, A.; Kim, H.; Gao, J.; Tang, J.; Hahn, H. T.; Chou, T. -W.; Itkis, M. E.; Haddon, R. C. *Langmuir* **2007**, *23*, 3970.
2. Sun, T.; Fan, H.; Zhuo, Q.; Liu, X.; Wu, Z. *High Perform. Polym.* **2014**, *26*, 892.
3. Uschitsky, M.; Suhir, E. *J. Electron. Packag.* **2001**, *123*, 47.
4. Wang, K.; Chen, L.; Wu, J.; Toh, M. L.; He, C.; Yee, A. F. *Macromolecules* **2005**, *38*, 788.
5. Wetzel, B.; Rosso, P.; Haupert, F.; Friedrich, K. *Eng. Fract. Mech.* **2006**, *73*, 2375.
6. Glaskova, T.; Aniskevich, A. *Compos. Sci. Technol.* **2009**, *69*, 2711.
7. Hammond, C. L.; Carroll, J. R. Environmental effects on composites, in AIAA/ASME 19th Structures, Structural Dynamics and Materials Conference, Paper 78–498 (1978), pp 270–274.
8. Hong, T. P.; Lesaint, O.; Gonon, P. *IEEE Trans. Dielectr. Electr. Insul.* **2009**, *16*, 1.
9. Lu, M. G.; Shim, M. J.; Kim, S. W. *J. Appl. Polym. Sci.* **2001**, *81*, 2253.
10. Zhao, H.; Li, R. K. Y. *Compos., Part A* **2008**, *39*, 602.
11. Pride, R. A. Environmental effects on composites for aircraft, 1978. Nasa Technical Memorandum 78716.
12. Anderson, I. *Antennas Propag.* **1975**, *23*, 619.
13. Blevis, B. *IEEE Trans. Antennas Propag.* **1965**, *13*, 175.
14. Kurri, M.; Huuskonen, A. *J. Atmos. Oceanic Technol.* **2008**, *25*, 1590.
15. Alexandre, M.; Dubois, P. *Mater. Sci. Eng., R* **2000**, *28*, 1.
16. Liu, W.; Hoa, S. V.; Pugh, M. *Compos. Sci. Technol.* **2008**, *68*, 2066.
17. Vertuccio, L.; Sorrentino, A.; Guadagno, L.; Bugatti, V.; Raimondo, M.; Naddeo, C.; Vittoria, V. *J. Polym. Res.* **2013**, *20*, 1.
18. Chen, B.; Liu, J.; Chen, H.; Wu, J. *Chem. Mater.* **2004**, *16*, 4864.
19. Blanton, T. N.; Majumdar, D.; Melpolder, S. M. *Mater. Res. Soc. Symp. Proc.* **2000**, *628*CC11.1 doi:10.1557/PROC-628-CC11.1.
20. Chin, I.-J.; Thurn-Albrecht, T.; Kim, H.-C.; Russell, T. P.; Wang, J. *Polymer* **2001**, *42*, 5947.
21. Oh, T.-K.; Hassan, M.; Beatty, C.; El-Shall, H. *J. Appl. Polym. Sci.* **2006**, *100*, 3465.
22. Fothergill, J.; Nelson, J. K.; Fu, M. Dielectric Properties of Epoxy Nanocomposites containing TiO2, Al2O3 and ZnO fillers, In Conference on Electrical Insulation and Dielectric Phenomena, **2004**, p 406. Boulder, Colorado.
23. Guevara-Morales, A.; Taylor, A. C. *J. Mater. Sci.* **2014**, *49*, 1574.
24. Imai, T.; Hirano, Y.; Hirai, H.; Kojima, S.; Shimizu, T. Preparation and Properties of Epoxy-Organically Modified Layered Silicate Nanocomposites, In IEEE International Symposium on Electrical Insulation, 2002. Boston, Massachusetts.
25. Katayama, J.; Ohki, Y.; Fuse, N.; Kozako, M.; Tanaka, T. *IEEE Trans. Dielectr. Electr. Insul.* **2013**, *20*, 157.
26. Imai, T.; Sawa, F.; Ozaki, T.; Shimizu, T.; Kido, R.; Kozako, M.; Tanaka, T. *IEEE Trans. Dielectr. Electr. Insul.* **2006**, *13*, 445.
27. Singha, S.; Thomas, M. J. *IEEE Trans. Dielectr. Electr. Insul.* **2008**, *15*, 12.
28. Abacha, N. Kubouchi, M.; Sakai, T.; Tsuda, K. *J. Appl. Polym. Sci.* **2009**, *112*, 1021.
29. Chen, C.; Curliss, D. *Nanotechnology* **2003**, *14*, 643.
30. Kim, J.-K.; Hu, C.; Woo, R. S. C.; Sham, M.-L. *Compos. Sci. Technol.* **2005**, *65*, 805.
31. Choi, I.; Kim, J. G.; Lee, D. G.; Seo, I. S. *Compos. Sci. Technol.* **2011**, *71*, 1632.
32. Reeder, J. Damage Tolerant Sandwich Panel Core With Low Moisture Affinity. In American Society for Composites 29th Technical Conference on Composite Materials, **2014**. San Diego, California.
33. Yasmin, A.; Abot, J. L.; Daniel, I. M. *Scr. Mater.* **2003**, *49*, 81.
34. Jeon, H. S.; Rameshwaram, J. K.; Kim, G. *J. Polym. Sci., Part B: Polym. Phys.* **2004**, *42*, 1000.
35. Filippi, S.; Paci, M.; Polacco, G.; Dintcheva, N. T.; Magagnini, P. *Polym. Degrad. Stab.* **2011**, *96*, 823.
36. Krupka, J.; Gregory, A. P.; Rochard, O. C.; Clarke, R. N.; Riddle, B.; Baker-Jarvis, J. *J. Eur. Ceram. Soc.* **2001**, *21*, 2673.
37. Agilent Technologies, Agilent Split Post Dielectric Resonators for Dielectric Measurements of Substrates, **2006**, Agilent Technologies.
38. Pontefisso, A.; Zappalorto, M.; Quaresimin, M. *Mech. Res. Commun.* **2013**, *52*, 92.